Dalton Transactions

Accepted Manuscript

ROYAL SOCIETY OF CHEMISTRY

www.rsc.org/dalton

Dalton Transactions

ARTICLE

Merging Open Metal Sites and Lewis Basic Sites in a NbO-type Metal-Organic Framework for Improved C_2H_2/CH_4 and CO_2/CH_4 Separation

Received 00th January 20xx,
Accepted 00th January 20xx

DOI: 10.1039/x0xx00000x

www.rsc.org/

Chengling Song,[a] Jiayi Hu, [a] Yajing Ling,[a] Yunlong Feng,[a] De-Li Chen,[b]* and Yabing He[a*]

A new three-dimensional NbO-type porous metal-organic framework **ZJNU-47** was synthesized *via* a solvothermal reaction of $Cu(NO_3)_2{\cdot}3H_2O$ and a Lewis basic nitrogen donor site-rich tetracarboxylate, namely, 5,5'-(pyridazine-3,6-diyl)-diisophthalate, and the structure was characterized by single-crystal X-ray diffraction to be isostructural with **NOTT-101**. With the synergistic effect of open metal sites, Lewis basic sites and suitable pore space, the MOF material **ZJNU-47a** after activation can take up a large amount of C_2H_2 and CO_2. The gravimetric C_2H_2 uptake of 214 cm^3 (STP) g^{-1} at room temperatue and 1 atm is the highest among all reported MOFs, and the gravimetric CO_2 uptake of 108 cm^3 (STP) g^{-1} is also among the highest reported for MOFs. Compared to the isostructural MOF **NOTT-101a**, **ZJNU-47a** exhibits a significant increase in C_2H_2 and CO_2 uptakes, and thus improved C_2H_2/CH_4 and CO_2/CH_4 separations. Significantly, the comprehensive DFT studies of C_2H_2 and CO_2 adsorption have revealed that the open nitrogen donor sites are comparable and even superior to open metal sites regarding to the adsorption sites. This work demonstrated that simultaneous introduction of Lewis basic nitrogen donor sites and Lewis acidic metal sites into the framewotrk is a promising approach to improve the gas sorption toward CO_2 and C_2H_2 and thus to produce materials with enhanced C_2H_2/CH_4 and CO_2/CH_4 separation performance.

Introduction

Acetylene is an important molecule that is widely used as a starting material for the synthesis of various organic compounds. Acetylene produced by thermal cracking of methane often contains unconverted methane. Therefore, efficient separation of C_2H_2 from CH_4 has become an important issue. On the other hand, separation of CO_2 from CH_4 is also an important industrial process for natural gas purification because the coexistence of CO_2 with CH_4 reduces the energy content of natural gas and can lead to pipeline corrosion. To meet pipeline requirements, natural gas must comply with strict CO_2 concentration limits. Since the traditional cryogenic distillation for such two separations, which is based on the different vapour pressures and thus boiling points of the constituents, is energy-intensive, the energy-efficient adsorption has been considered an attractive method. Thus, porous materials that can efficiently separate C_2H_2/CH_4 and CO_2/CH_4 mixtures are urgently necessary.

Metal-organic frameworks (MOFs), assembled from inorganic metal ions/clusters (generally termed as secondary building units (SBUs)) and multidentate organic bridging ligands *via* metal coordination bonds, have been rapidly emerging as a new kind of porous materials. The modular assembly nature and mild synthetic conditions allow their pore sizes and shapes to be systematically tuned by the judicious choice of metal-containing SBUs and bridging linkers. Furthermore, some functional sites such as open metal sites (OMSs) and organic functional groups can be immobilized in the pore surface affording specific binding sites that can selectively recognize the target molecules. Such attractive features offer a great promise for their potential applications in gas storage and separation.[1] In fact, many research on porous MOFs has demonstrated their enormous potential for diverse gas separations such as separation of CO_2/CH_4,[2] light hydrocarbons,[3] noble gases,[4] and hexane isomers.[5]

To increase the gas uptake capacities of MOFs towards CO_2 and C_2H_2, current efforts are largely devoted to enhancing the binding affinity of C_2H_2 and CO_2 in the MOFs. Immobilization of OMSs within pore surface of MOFs is one commonly used strategy because neutron powder diffraction (NPD) and inelastic neutron scattering (INS) studies have verified that in most cases, one OMS binds one C_2H_2 or CO_2 molecule.[6] MOF-74 series can serve as excellent examples.[6b, 7] Besides, one of the ongoing endeavours is to functionalize the organic linkers with some specific binding sites and improve the interactions

[a] College of Chemistry and Life Sciences, Zhejiang Normal University, Jinhua 321004, China. E-mail: heyabing@zjnu.cn.
[b] Key Laboratory of the Ministry of Education for Advanced Catalysis Materials, Institute of Physical Chemistry, Zhejiang Normal University, 321004 Jinhua, China. E-mail: chendl@zjnu.cn

Electronic Supplementary Information (ESI) available: PXRD pattern (Fig. S1), TGA (Fig. S2), N_2 adsorption-desorption isotherm (Fig. S3), BET and Langmuir plots (Fig. S4), FTIR spectra (Fig. S5), NMR spectra (Fig. S6), crystal data and structure refinement for **ZJNU-47** (Table S1). CCDC 1056733. For ESI and crystallographic data in CIF or other electronic format See DOI: 10.1039/x0xx00000x

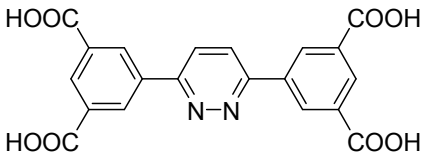

Scheme 1 The organic building block H_4L used to construct the metal-organic framework **ZJNU-47**.

between the framework and C_2H_2/CO_2 molecules. Reported strategies include amine grafting,[8] and introducing strongly polarizing functional groups.[9] For example, we recently reported that functionalization of the organic linker, 1,4-benzenediisophthalate, in **NOTT-101**[10] with highly polarized benzothiadiazole moieties can dramatically improve CO_2 uptake capacities and adsorption selectivities towards CO_2 over CH_4 and N_2.[9] Naturally, simultaneous immobilization of OMSs and organic functional sites in the pore surface will be expected to significantly improve the C_2H_2/CH_4 and CO_2/CH_4 separations. In this regard, some progress has been made,[11] but the MOFs with both high uptake capacities of C_2H_2 and CO_2 and excellent adsorption selectivities toward C_2H_2 and CO_2 over CH_4 have not been revealed.

Based on the above considerations, in the work, we modified the organic linker, 1,4-benzenediisophthalate, in **NOTT-101**[10] by replacing the benzene ring with pyridazine ring that has high density of Lewis basic nitrogen sites, and targeted the corresponding NbO-type MOF, which we termed **ZJNU-47**. Amazingly, at room temperature and 1 atm, the activated **ZJNU-47a** (thereafter, the letter "a" indicates activated MOF materials) exhibits the highest gravimetric C_2H_2 uptake among all reported MOFs.[12] Also, the gravimetric CO_2 uptake at room temperature and 1 atm is among the highest MOFs reported up to date.[12a] Furthermore, compared to the isostructural **NOTT-101a**, the activated **ZJNU-47a** exhibits a significant increase in C_2H_2 and CO_2 uptakes, and thus improved C_2H_2/CH_4 and CO_2/CH_4 separations.

Experimental

Materials and Measurements

All starting materials and reagents for synthesis were commercially available and used as received. ^{1}H NMR and ^{13}C NMR spectra were recorded on a Bruke Avance 600 spectrometer. Fourier transform infrared (FTIR) spectrum was recorded using a Nicolet 5DX FT-IR spectrometer. Thermogravimetric analyses (TGA) were carried out using a Netzsch STA 449C thermal analyzer with a heating rate of 5 k min^{-1} in a flowing nitrogen atmosphere (10 mL min^{-1}). Powder X-ray diffraction (PXRD) patterns were recorded on a Philips PW3040/60 automated powder diffractometer, using Cu-K_α radiation (λ = 1.542 Å) with a 2θ range of 5-35°. The elemental analyses were performed with a Perkin–Elmer 240 CHN analyzer. A Micromeritics ASAP 2020 surface area analyser was used to measure gas adsorption isotherms. To have a guest–free framework, the fresh sample was guest-exchanged with dry acetone at least 10 times, filtered and evacuated under vacuum at 373 K until the outgas rate was 6 μmHg min^{-1} prior to measurements. A sample of 55.0 mg was used for the sorption measurements and was maintained at 77 K with liquid nitrogen, and at 273 K with an ice-water bath. As the center-controlled air conditioner was set up at 296 K, a water bath was used for adsorption isotherms at 296 K.

X-ray Crystallography

The X-ray diffraction data were collected on a Agilent supernova dual diffractometer with Mo-K_a radiation (λ = 0.71073 Å). Absorption corrections were performed using a multi-scan method. The structure was solved by direct methods with SHELXS-97[13] and refined with a full-matrix least-squares technique within the SHELXL program package. The unit cell includes a large region of disordered solvent molecules, which could not be modelled as discrete atomic sites. We employed PLATON/SQUEEZE[14] to calculate the diffraction contribution of the solvent molecules and, thereby, to produce a set of solvent-free diffraction intensities; structures were then refined again using the data generated. Hydrogen atoms of the ligand were calculated in ideal positions with isotropic displacement parameters, while H atoms of water molecules were not included in the final refinement. The crystal data and structure refinement results are listed in Table S1 in the Supporting Information. The CCDC reference number is 1056733. The supplementary crystallographic data for the compound can be obtained free of charge from the Cambridge Crystallographic Data Centre *via* http://www.ccdc.cam.ac.uk/data_request/cif.

Quantum Chemical Calculations

All of the periodic density functional theory (DFT) calculations were performed in Vienna ab initio simulation package.[15] The van der Waals (vdW) corrected DFT method, vdW-DF2,[16] has been successfully used to reproduce weak van der Waals in many systems,[17] and thus is able to reproduce the vdW energies between the gas molecules (C_2H_2, CO_2, and CH_4) and **ZJNU-47** framework. The Brillouin zone was sampled with gamma point only, which is sufficient for the calculations of binding energies since the values are almost unchanged by increasing Monkhorst-Pack grids[18] wherein all of our calculations a planewave energy cutoff of 500 eV was employed. The crystal unit cell of **ZJNU-47a** consists of 360 atoms, which is further reduced to a primitive cell ($a = b = c$ = 16.61 Å, $\alpha = \beta = \gamma = 68.76^o$) with 120 atoms for the sake of computational efficiency. The lattice constants are fixed while all of the atoms were allowed to relax using vdW-DF2. For the optimizations of adsorbates/**ZJNU-47a**, all of the atoms were relaxed until the force on each ion was less than 0.005 eV $Å^{-1}$. More details on the accuracy of our calculations are available in Supporting Information.

Synthesis and Characterization of the Organic Linker H_4L

To a mixture of 3,6-dibromopyridazine (1.00 g, 4.20 mmol), dimethyl 5-(pinacolboryl)isophthalate (2.96 g, 9.25 mmol), Cs_2CO_3 (4.11 g, 12.61 mmol) and $Pd(PPh_3)_4$ (0.24 g, 0.21 mmol) was added dry dioxane (100 mL). The resulting mixture was stirred under reflux under a nitrogen atmosphere for 72 h. After removal of the solvents, CH_2Cl_2 (100 mL) and H_2O (80 mL)

were added. The mixture was filtered through Celite. The organic phase was separated and the water phase was extracted with CH_2Cl_2 (50 mL×3). The combined organic phase was washed with brine (80 mL), dried over anhydrous $MgSO_4$ and filtered. Volatiles were removed by rota-evaporation under reduced pressure, and the obtained residue was purified with silica gel column chromatography using petroleum ether/CH_2Cl_2/ethyl acetate (4/4/1, *v*/*v*/*v*) as eluent, affording the tetramethyl intermediate as a white solid (1.27 g, 2.73 mmol, 65%). ^{1}H NMR ($CDCl_3$, 600.1 MHz) δ (ppm): 9.110 (d, J = 1.2 Hz, 4H), 8.874 (t, J = 1.2 Hz, 2H), 8.173 (s, 2H), 4.043 (s, 12H).

To a suspension of the tetramethyl intermediate (1.27 g, 2.73 mmol) in THF (20 mL) and MeOH (20 mL) was added 6 M NaOH (20 mL, 120 mmol). The resulting mixture was refluxed overnight. After removal of the solvents, the residue was dissolved in water, and acidified with conc. HCl at 273 K. The precipitation was collected by filtration, and dried in vacuum at 343 K to afford the target compound in quantitative yield. ^{1}H NMR (DMSO-d_6, 600.1 MHz) δ (ppm): 8.952 (s, 4H), 8.628 (s, 2H), 8.524 (s, 2H); ^{13}C NMR (DMSO-d_6, 150.9 MHz) δ (ppm): 167.130, 156.825, 136.817, 133.602, 131.741, 131.473, 125.900; Selected FTIR (KBr, cm^{-1}): 1718, 1389, 1273, 1246, 758, 679.

Synthesis and Characterization of ZJNU-47

A mixture of the organic linker H_4L (5.0 mg, 10.77 μmol) and $Cu(NO_3)_2{\cdot}3H_2O$ (15.0 mg, 62.10 μmol) was dissolved into a mixed solvent of *N*,*N*-dimethylformamide (DMF), ethanol and H_2O (1.5 mL / 0.5 mL / 0.08 mL) in a screw-capped vial (20 mL). 50 μL of 6 M HCl were then added. The vial was capped and heated at 353 K for 96 h. Blue rhombic crystals were obtained in 63% yield. Based on single-crystal X-ray determination, TGA, and microanalysis, **ZJNU-47** can be best formulated as $[Cu_2L(H_2O)_2]{\cdot}3DMF{\cdot}3EtOH{\cdot}2H_2O$. Selected FTIR (KBr, cm^{-1}): 2929, 1655, 1450, 1381, 1300, 1254, 1095, 1061, 1049, 926, 854, 775, 760, 729, 661, 488; anal. for $C_{35}H_{55}Cu_2N_5O_{18}$, calcd: C, 43.75%, H, 5.77%, N, 7.29%; found: C, 43.82%, H, 5.65%, N, 7.21%.

Results and Discussion

Synthesis and Characterization

The organic linker, 5,5′-(pyridazine-3,6-diyl)-diisophthalate (H_4L), was readily synthesized using palladium-catalyzed Suzuki cross-coupling reaction of 3,6-dibromopyridazine and 5-(pinacolbory)isophthalate followed by hydrolysis and acidification in good yield and gram scale. The detailed procedure was provided in Experimental Section. The ligand was characterized ambiguously by ^{1}H and ^{13}C NMR spectra.

ZJNU-47 was obtained as blue block-shaped crystals, which are insoluble in common organic solvents, *via* a solvothermal reaction of the organic linker H_4L and $Cu(NO_3)_2{\cdot}3H_2O$ in a mixed solvent of *N*,*N*-dimethylformamide (DMF), EtOH and H_2O with the addition of a small amount of hydrochloric acid at 353 K for 96 h. The structure was characterized by single-crystal X-ray diffraction studies, and the phase purity of the bulk material was confirmed by a good match between the powder X-ray diffraction (PXRD, Fig. S1 in the Supporting Information) and the one simulated from its single-crystal X-ray diffraction structure. Thermogravimetric analysis (TGA, Fig. S2) showed that **ZJNU-47** lost a large amount of solvent molecules in the temperature below 553 K, and above this temperature, started to decompose rapidly. Based on single-crystal X-ray diffraction studies, TGA, and elemental microanalysis, the formula of **ZJNU-47** was determined to be $[Cu_2(L)(H_2O)_2]{\cdot}3DMF{\cdot}3EtOH{\cdot}2H_2O$.

Structural Description

Single-crystal X-ray diffraction analysis reveals that **ZJNU-47** crystallizes in a trigonal space group of *R*-3m with unit cell edge lengths of a = b = 18.7626(3) Å and c = 37.7902(14) Å. The framework is composed of paddlewheel dicopper $Cu_2(COO)_4$ SBUs which are connected by organic linkers to form a three-dimensional (3D) NbO-type structure in which both the $Cu_2(COO)_4$ SBUs and the organic linkers are taken as planar 4-connected nodes (Fig. 1). Alternatively, if the bridging organic linker is considered as having two 3-coordinated (3-c) branch points, then in combination with the 4-coordinated dicopper paddlewheels, the derived net is the one with the RCSR symbol fof.[19] In the framework, there exist two different types of cages, one of which, indicated by blue sphere in Fig. 1b, is composed of 12 ligands connecting 6 paddlewheel SBUs, and the other one, indicated by green sphere in Fig. 1b, is formed from 6 ligands connecting 12 paddlewheel SBUs. Taking into account of van der Waals radii of the atoms, the dimensions of the two cages are *ca.* 11 Å and 12 × 21 Å^2 in diameter, respectively. The nitrogen atoms in the spacer between two terminal isophthalate moieties did not participate in the coordination with Cu^{2+} ions, affording additional gas binding sites for electron acceptor gas molecules. Thus, two cages were decorated with abundant Lewis basic nitrogen donor sites and Lewis acidic unsaturated copper sites after removal of the terminal water molecules. PLATON analysis reveals the total accessible volume in **ZJNU-47** is 67.5% of the volume of the unit cell when the disordered

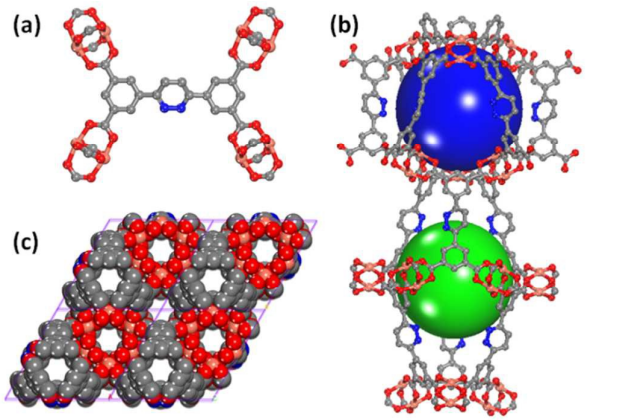

Fig. 1 (a) The coordination environment of the organic linker; (b) two different types of polyhedral nanocages; and (c) CPK representation of a three-dimensional open framework viewed along the *c* direction. The hydrogen atoms were omitted for clarity.

solvent molecules and the terminal water molecules are removed (7774.1 Å^3 out of the 11521.2 Å^3 *per* unit cell volume).[20]

Permanent Porosity

To characterize the permanent porosity, the N_2 adsorption-desorption isotherm was collected at 77 K by using a Micromeritics ASAP 2020 surface area and pore size analyser. Before gas sorption measurements, the as-synthesized sample was washed with DMF and activated by solvent exchange with dry acetone followed by evacuation under dynamic vacuum at 373 K overnight, generating the activated sample **ZJNU-47a**. As shown in Fig. S3 in the supporting information, the activated **ZJNU-47a** exhibits reversible Type-I sorption behaviour, characteristic of microporous materials. At relative pressure P/P_o of 0.96, the N_2 sorption amount reach 690 cm^3 (STP) g^{-1}. The Brunauer–Emmett–Teller (BET) surface area was calculated using BET equation from the adsorption branch of the nitrogen isotherm over a relative pressure range of P/P_o = 0.01-0.04, and was found to be 2703 m^2 g^{-1} (Fig. S3). The overall Langmuir surface area calculated using the Langmuir equation from the N_2 sorption isotherm over the entire pressure range is 2961 m^2 g^{-1} (Fig. S3). The pore volume calculated from the maximum amount of N_2 adsorbed is 1.07 cm^3 g^{-1}, which is in good agreement with the calculated value of 1.02 cm^3 g^{-1} by PLATON. These values are comparable to those of **NOTT-101a** that is built from terphenyl-3,3',5,5'-tetracarboxylic acid of the same length as H_4L.[10]

C_2H_2, CO_2 and CH_4 Adsorption

Considering that **ZJNU-47a** combines Lewis acidic open copper sites and Lewis basic nitrogen donor sites in the framework suitable for C_2H_2/CH_4 and CO_2/CH_4 separations, the C_2H_2, CO_2, CH_4 sorption isotherms were measured systematically at two different temperatures of 273 K and 296 K up to 1 atm accordingly. As shown in Fig. 2, all isotherms are completely reversible and show no hysteresis.

The activated **ZJNU-47a** can take up 300 cm^3 (STP) g^{-1} of C_2H_2 at 273 K at 1 atm, which decreases to 214 cm^3 (STP) g^{-1} when the temperature increased to 296 K. The C_2H_2 uptake is still not saturated, which means that the C_2H_2 uptake can be further maximized until the limit of safe storage of C_2H_2 under a pressure of 0.2 MPa. To the best of our knowledge, the gravimetric C_2H_2 uptake at room temperature and 1 atm is the highest among all reported MOFs up to date under the same conditions: NOTT-109 (204 cm^3 (STP) g^{-1})[12a], HKUST-1 (201 cm^3 (STP) g^{-1})[6a], CoMOF-74 (197 cm^3 (STP) g^{-1})[6b], Cu_2(ebtc) (160 cm^3 (STP) g^{-1}, ebtc = 1,1'-ethynebenzene-3,3',5,5'-tetracarboxylate)[21], [Cu_4L] (154 cm^3 (STP) g^{-1}, L = tetrakis[(3,5-dicarboxyphenoxy)methyl] methane)[22], MOF-505 (148 cm^3 (STP) g^{-1})[6a]. The storage density of C_2H_2 of 0.232 g cm^{-3} is equivalent to the acetylene density at 22.1 MPa and 110 times greater than the compression limit for the safe storage of C_2H_2 (0.2 MPa).

At 1 atm, **ZJNU-47a** exhibits CO_2 uptakes of 108 cm^3 (STP) g^{-1} and 169 cm^3 (STP) g^{-1} at 296 K and 273 K, respectively. The gravimetric CO_2 adsorption capacity at room temperature and 1 atm is also among the highest reported for isoreticular Cu-based MOFs: ZJNU-40 (108 cm^3 (STP) g^{-1})[9], NJU-Bai14 (100 cm^3 (STP) g^{-1})[23], NOTT-125a(92.59 cm^3 (STP) g^{-1})[24], MOF-505 (73 cm^3 (STP) g^{-1})[25].

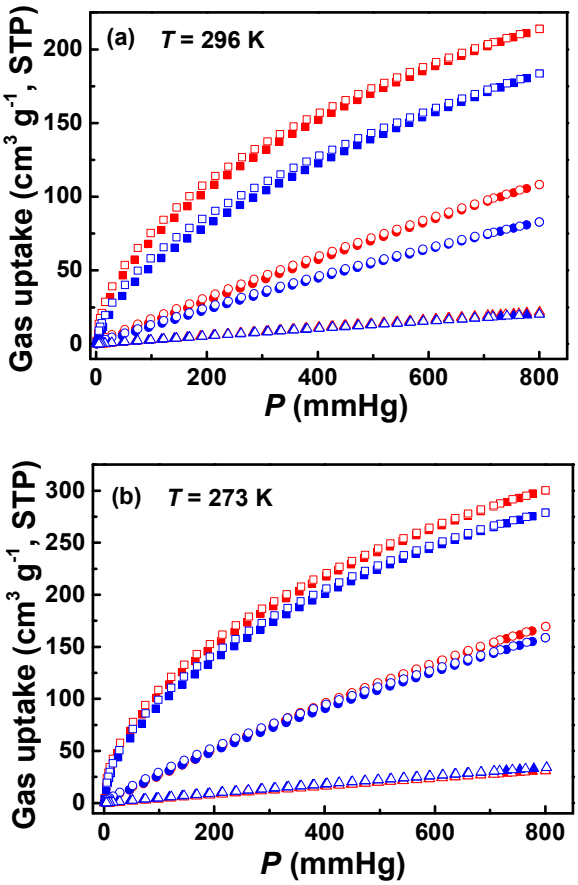

Fig. 2 C_2H_2 (square), CO_2 (circle) and CH_4 (triangle) sorption isotherms of **ZJNU-47a** (red) and **NOTT-101a** (blue) at 296 K (a) and 273 K (b). Solid and open symbols represent adsorption and desorption, respectively. STP = Standard Temperature and Pressure.

In sharp contrast to CO_2 and C_2H_2, **ZJNU-47a** can absorb only limited amounts of CH_4. The CH_4 uptake capacities at 1 atm are 31.0 and 21.8 cm^3 (STP) g^{-1} at 273 K and 296 K, respectively. Such a discrimination of adsorption capacities enables **ZJNU-47a** to be a promising material for the selective separation of C_2H_2-CH_4 and CO_2-CH_4 gas mixtures. More importantly, compared to the isostructural MOF **NOTT-101a**, **ZJNU-47a** exhibits a significant increase in C_2H_2 and CO_2 uptakes (Fig. 2), indicating the introduction of Lewis basic nitrogen atoms into the framework of the same structure can dramatically boost C_2H_2 and CO_2 gas uptake capacities, and thus improve C_2H_2/CH_4 and CO_2/CH_4 separations.

Quantum Chemical Calculations

To probe the favourable adsorption sites for C_2H_2, CO_2, and CH_4, many different configurations have been built as initial structures for optimization using vdW-DF2 method. Fig. 3 shows different adsorption sites for C_2H_2 and CO_2 in **ZJNU-47a**, as well as their binding energies (E_b). Note that the binding

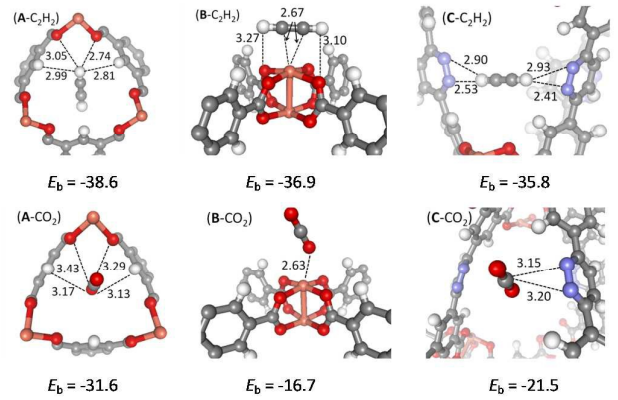

Fig. 3 Several optimized structures representing the typical adsorption sites for C_2H_2 and CO_2 in **ZJNU-47a** material are shown, together with several bond lengths and vdW-DF2 computed binding energy for each configuration. The units for bond distance and binding energy are Å and kJ mol^{-1}, respectively.

energy is calculated as:

$$E_b = E_{gas/ZJNU-47a} - E_{gas} - E_{ZJNU-47a}$$

where $E_{gas/ZJNU-47a}$, E_{gas}, and $E_{ZJNU-47a}$ represent the energies for gas adsorbed **ZJNU-47a**, isolated gas, and pure **ZJNU-47a** material, respectively. For clarity, only a few of atoms surrounding the gas molecule are shown in Fig. 3 to represent the periodic structure. Interestingly, the most favourable adsorption site for C_2H_2 is right at the window connecting the two adjacent cages, labelled as site "A-C_2H_2" in Fig. 3, with E_b of -38.6 kJ mol^{-1}. The acetylene molecule is encapsulated by the window and thus several strong hydrogen bonds (see A-C_2H_2 in Fig. 3) between H atom (acetylene) and atoms at the window (oxygen and hydrogen atoms) are formed, leading to a strong binding energy. The open metal site (site B) also has a strong binding affinity for C_2H_2 with E_b = -36.9 kJ mol^{-1}, with both C-Cu bond lengths of 2.67 Å. Another interesting binding site for C_2H_2 is labelled as site C (open nitrogen site), bridging the two neighbouring L^{4-} ligands. As shown in Fig. 3, the C_2H_2 molecule sits at the center of two organic linkers and the formed configuration of N···H—C≡C—H···N enables strong hydrogen bonding between acetylene molecule and two organic linkers, with four H···N bond lengths of 2.41, 2.53, 2.90, and 2.93 Å, respectively. It is intriguing that the vdW-DF2 computed binding energy of -35.8 kJ mol^{-1} is so large, which is even comparable to the E_b values, *i.e.*, -38.6 and -36.9 kJ mol^{-1}, at the other two sites A (window) and B (open metal site), respectively. This strong adsorption affinity arising only from organic linker might explain why **ZJNU-47a** has a very high storage capacity compared to other porous materials.

It is well known that many porous MOF materials with both open metal sites and nitrogen groups have high storage capacity for gases such as C_2H_2.[26] For example, Rao and co-workers found that the C_2H_2 storage capacity of 290 cm^3 (STP) g^{-1} at 273 K and 1 atm for **ZJU-5a** is the highest among the reported porous materials when it was reported.[26a] The **ZJU-5** material also has **nbo** topology and the organic linker is similar to the organic linker in **ZJNU-47**. The only difference is that there is only one nitrogen group in the organic linker of **ZJU-5**, while there is a double N-N group in the organic linker in **ZJNU-47**. To evaluate how the single N group in **ZJU-5** and double N-N group in **ZJNU-47** performs on binding C_2H_2, we also calculated the binding energy of C_2H_2 with a similar orientation to "C-C_2H_2" (Fig. 3) in **ZJU-5**. The results show that the E_b is -29.9 kJ mol^{-1} (see supporting information for computation details), weaker than that of "C-C_2H_2" by about 5.9 kJ mol^{-1}. This comparison confirms that the double N-N group in **ZJNU-47a** is energetically more favourable for binding C_2H_2 than the single N group in **ZJU-5a**, and thus well explain the phenomenon that **ZJNU-47a** has relatively larger storage capacity of 300 cm^3 (STP) g^{-1} at the same condition. Since these two porous materials have very similar structure, the larger adsorption affinity of C_2H_2 in **ZJNU-47a** is attributed to the stronger hydrogen bonding between the double N-N group and acetylene, and finally leads to large storage capacity. However, for the porous MOF materials with different topologies, different number of nitrogen groups and different sizes of cages, it is complicated to conclude which are the key factors to make the materials more effective on gas adsorption. Our combined experimental and theoretical work demonstrates that it is plausible to enhance the storage capacity by designing organic linkers *via* enhanced guest-host interactions.

Similar to C_2H_2, the site A is also the most favourable adsorption site (E_b = -31.6 kJ mol^{-1}) for CO_2. As shown in Fig. 3 (A-CO_2), the C atom in CO_2 is close to the two O atoms from paddle-wheeled subunit group, with C···O distances of 3.29 and 3.43 Å; also, there are two O···H bonds between CO_2 and the window, with distances of 3.13 and 3.17 Å. Interestingly, the open nitrogen site (C-CO_2) is the second favourable adsorption site for CO_2, with binding energy of -21.5 kJ mol^{-1}, stronger than that (-16.7 kJ mol^{-1}) of site B-CO_2 by 4.8 kJ mol^{-1}. This is a very interesting phenomenon since the open metal site was considered as an important adsorption site for CO_2, and our predicted results indicate that the open nitrogen sites in **ZJNU-47a** material play an important role in adsorption of CO_2.

The comprehensive DFT studies of C_2H_2 and CO_2 indicate that the open nitrogen sites are comparable and even superior to open metal sites regarding to the adsorption sites, and thus explain the experimental results that the **ZJNU-47a** has a larger loading for both C_2H_2 and CO_2 than **NOTT-101a** at the same condition. However, the open nitrogen sites in **ZJNU-47a** do not significantly improve the adsorption affinity of CH_4. Theoretical calculations indicate that the binding energies for CH_4 close to the open nitrogen sites are about 12 to 14 kJ mol^{-1}, much smaller than that (-17.6 kJ mol^{-1}) of open metal site and -30.1 kJ mol^{-1} at the window.

Conclusions

In summary, a nitrogen-rich organic building block was successfully incorporated into a new porous NbO-type metal-organic framework **ZJNU-47**, which is isostructural with **NOTT-101**. With the synergistic effect of the Lewis acidic open metal sites (1.56 nm^{-3}) and Lewis basic nitrogen donor sites (1.56 nm^{-}

^{3}) immobilized within the pore surfaces, the activated **ZJNU-47a** exhibited exceptionally high C_2H_2 and CO_2 uptakes of 214 and 108 cm^3 (STP) g^{-1} at room temperature under 1 atm, respectively. These values are among the highest reported for MOFs up to date. Compared to the isostructural MOF **NOTT-101a**, **ZJNU-47a** exhibits a significant increase in C_2H_2 and CO_2 uptakes, and thus improved C_2H_2/CH_4 and CO_2/CH_4 separations. Furthermore, the comprehensive DFT studies of C_2H_2 and CO_2 adsorption have revealed that the open nitrogen donor sites are comparable and even superior to open metal sites regarding to the adsorption sites. This work demonstrates simultaneous incorporation of Lewis acidic open metal sites and Lewis basic nitrogen donor sites into the framework provides a promising approach to improve the gas sorption toward C_2H_2 and CO_2 and thus to produce materials with enhanced C_2H_2/CH_4 and CO_2/CH_4 separation performance.

Acknowledgement

Y. He acknowledged financial support from the National Natural Science foundation of China (NSFC grant No. 21301156) and the support from Open Research Fund of Top Key Discipline of Chemistry in Zhejiang Provincial Colleges, and Key Laboratory of the Ministry of Education for Advanced Catalysis Materials (Zhejiang Normal University, ZJHX201313). D.-L Chen thanks financial support from the National Natural Science foundation of China (NSFC grant No. 21303165).

Reference

1 (a) J.-R. Li, J. Sculley and H.-C. Zhou, *Chem. Rev.*, 2012, **112**, 869-932; (b) H. Wu, Q. Gong, D. H. Olson and J. Li, *Chem. Rev.*, 2012, **112**, 836-868; (c) K. Sumida, D. L. Rogow, J. A. Mason, T. M. McDonald, E. D. Bloch, Z. R. Herm, T.-H. Bae and J. R. Long, *Chem. Rev.*, 2012, **112**, 724-781.
2 D. Britt, H. Furukawa, B. Wang, T. G. Glover and O. M. Yaghi, *Proc. Natl. Acad. Sci.*, 2009, **106**, 20637-20640.
3 (a) Y. He, R. Krishna and B. Chen, *Energy Environ. Sci.*, 2012, **5**, 9107-9120 ; (b) Y. He, Z. Zhang, S. Xiang, F. R. Fronczek, R. Krishna and B. Chen, *Chem. Eur. J.*, 2012, **18**, 613-619; (c) Y. He, Z. Zhang, S. Xiang, H. Wu, F. R. Fronczek, W. Zhou, R. Krishna, M. O'Keeffe and B. Chen, *Chem. Eur. J.*, 2012, **18**, 1901-1904; (d) E. D. Bloch, W. L. Queen, R. Krishna, J. M. Zadrozny, C. M. Brown and J. R. Long, *Science*, 2012, **335**, 1606-1610.
4 (a) J. J. P. IV, S. L. Teich-McGoldrick, S. T. Meek, J. A. Greathouse, M. Haranczyk and M. D. Allendorf, *J. Phys. Chem. C*, 2014, **118**, 11685-11698; (b) M. V. Parkes, C. L. Staiger, J. J. P. IV, M. D. Allendorf and J. A. Greathouse, *Phys. Chem. Chem. Phys.*, 2013, **15**, 9093-9106.
5 Z. R. Herm, B. M. Wiers, J. A. Mason, J. M. v. Baten, M. R. Hudson, P. Zajdel, C. M. Brown, N. Masciocchi, R. Krishna and J. R. Long, *Science*, 2013, **340**, 960-964.
6 (a) S. Xiang, W. Zhou, J. M. Gallegos, Y. Liu and B. Chen, *J. Am. Chem. Soc.*, 2009, **131**, 12415-12419; (b) S. Xiang, W. Zhou, Z. Zhang, M. A. Green, Y. Liu and B. Chen, *Angew. Chem. Int. Ed.*, 2010, **49**, 4615-4618; (c) P. D. C. Dietzel, R. E. Johnsen, H. Fjellvåg, S. Bordiga, E. Groppo, S. Chavan and R. Blom, *Chem. Commun.*, 2008, 5125-5127.
7 S. R. Caskey, A. G. Wong-Foy and A. J. Matzger, *J. Am. Chem. Soc.*, 2008, **130**, 10870-10871.
8 (a) J. An, S. J. Geib and N. L. Rosi, *J. Am. Chem. Soc.*, 2010, **132**, 38-39; (b) B. Li, Z. Zhang, Y. Li, K. Yao, Y. Zhu, Z. Deng, F. Yang, X. Zhou, G. Li, H. Wu, N. Nijem, Y. J. Chabal, Z. Lai, Y. Han, Z. Shi, S. Feng and J. Li, *Angew. Chem. Int. Ed.*, 2012, **51**, 1412-1415.
9 C. Song, Y. He, B. Li, Y. Ling, H. Wang, Y. Feng, R. Krishna and B. Chen, *Chem. Commun.*, 2014, **50**, 12105-12108.
10 X. Lin, J. Jia, X. Zhao, K. M. Thomas, A. J. Blake, G. S. Walker, N. R. Champness, P. Hubberstey and M. Schröder, *Angew. Chem. Int. Ed.*, 2006, **45**, 7358-7364.
11 H. Xu, Y. He, Z. Zhang, S. Xiang, J. Cai, Y. Cui, Y. Yang, G. Qian and B. Chen, *J. Mater. Chem. A*, 2013, **1**, 77-81.
12 (a) Y. He, B. Li, M. O'Keeffe and B. Chen, *Chem. Soc. Rev.*, 2014, **43**, 5618-5656; (b) Y. He, W. Zhou, R. Krishna and B. Chen, *Chem. Commun.*, 2012, **48**, 11813-11831; (c) Z. Zhang, S. Xiang and B. Chen, *CrystEngComm*, 2011, **13**, 5983-5992.
13 G. M. Sheldrick, Acta Crystallogr. Sect. A, 2008, 64, 112.
14 A. L. Spek, J. Appl. Crystallogr., 2003, 36, 7.
15 (a) G. Kresse, *J. Non-Cryst. Solid*, 1995, **193**, 222-229; (b) G. Kresse and J. Hafner, *Phys. Rev. B*, 1994, **49**; (c) G. Kresse and J. Furthmüller, *Phys. Rev. B*, 1996, **54**, 11169 ; (d) G. Kresse and J. Furthmüller, *Comput. Mater. Sci.*, 1996, **6**, 15-50.
16 (a) J. Klimeš, D. R. Bowler and A. Michaelides, *J. Phys.: Cond. Mat.*, 2010, **22**, 022201; (b) J. Klimeš, D. R. Bowler and A. Michaelides, *Phys. Rev. B*, 2011, **83**, 195131.
17 (a) M. K. Rana, H. S. Koh, J. Hwang and D. J. Siegel, *J. Phys. Chem. C*, 2012, **116**, 16957-16968; (b) D.-L. Chen, L. Mandeltort, W. A. Saidi, J. John T. Yates, M. W. Cole and J. K. Johnson, *Phys. Rev. Lett.*, 2013, **110**, 135503; (c) L. Mandeltort, D.-L. Chen, W. A. Saidi, J. K. Johnson, M. W. Cole and J. John T. Yates, *J. Am. Chem. Soc.*, 2013, **135**, 7768-7776.
18 H. J. Monkhorst and J. D. Pack, *Phys. Rev. B*, 1976, **13**, 5188.
19 M. O'Keeffe and O. M. Yaghi, *Chem. Rev.*, 2012, **112**, 675-702.
20 Spek, A. L. Acta Crystallogr., Sect. D 2009, 65, 148−155.
21 Y. Hu, S. Xiang, W. Zhang, Z. Zhang, L. Wang, J. Bai and B. Chen, *Chem. Commun.*, 2009, 7551-7553.
22 Y.-S. Xue, Y. He, S.-B. Ren, Y. Yue, L. Zhou, Y.-Z. Li, H.-B. Du, X.-Z. You and B. Chen, *J. Mater. Chem.*, 2012, **22**, 10195-10199.
23 M. Zhang, Q. Wang, Z. Lu, H. Liu, W. Liu and J. Bai, *CrystEngComm*, 2014, **16**, 6287-6290.
24 N. H. Alsmail, M. Suyetin, Y. Yan, R. Cabot, C. P. Krap, J. Lü, T. L. Easun, E. Bichoutskaia, W. Lewis, A. J. Blake and M. Schröder, *Chem. Eur. J.*, 2014, **20**, 7317-7324.
25 A. R. Millward and O. M. Yaghi, *J. Am. Chem. Soc.*, 2005, **127**, 17998-17999.
26 (a) X. Rao, J. Cai, J. Yu, Y. He, C. Wu, W. Zhou, T. Yildirim, B. Chen and G. Qian, *Chem. Commun.*, 2013, **49**, 6719-6721; (b) K. Liu, B. Li, Y. Li, X. Li, F. Yang, G. Zeng, Y. Peng, Z. Zhang, G. Li, Z. Shi, S. Feng and D. Song, *Chem. Commun.*, 2014, **50**, 5031-5033; (c) K. Liu, D. Ma, B. Li, Y. Li, K. Yao, Z. Zhang, Y. Han and Z. Shi, *J. Mater. Chem. A*, 2014, **2**, 15823-15828.
27

Graphical abstract

A new NbO-type metal-organic framework **ZJNU-47a** incorporating Lewis acidic copper sites and Lewis basic nitrogen donor sites exhibits the better performance than the isostructural NOTT-101a for the separation of C_2H_2/CH_4 and CO_2/CH_4 gas mixtures at room temperature.